

Characterisation of Materials Used in Flex Bearings of Large Solid Rocket Motors

CH.V. Ram Mohan*, J. Ramanathan, Satish Kumar#, and A.V.S.S.K.S. Gupta†

* *Advanced Systems Laboratory, Hyderabad*

Terminal Ballistics Research Laboratory, Chandigarh

† *Jawaharlal Nehru Technological University, Hyderabad*

*E-mail: rammohanchv66123@rediffmail.com

ABSTRACT

Solid rocket motors are propulsion devices for both satellite launchers and missiles, which require guidance and steering to fly along a programmed trajectory and to compensate for flight disturbances. A typical solid rocket motor consists of motor case, solid propellant grain, motor insulation, igniter and nozzle. In most solid rocket motors, thrust vector control (TVC) is required. One of the most efficient methods of TVC is by flex nozzle system. The flex nozzle consists of a flexible bearing made of an elastomeric material alternating with reinforcement rings of metallic or composite material. The material characterisation of AFNOR 15CDV6 steel and the natural rubber-based elastomer developed for use in flex nozzle are discussed. This includes testing, modelling of the material, selection of a material model suitable for analysis, and the validation of material model.

Keywords: Flex bearing, Mooney-Rivlin model, Ogden model, Yeoh model, tensile testing, quadruple lap shear specimen

NOMENCLATURE

W	Strain energy potential
\bar{I}_1, \bar{I}_2	Strain invariants
d	Material compressibility parameter
K	Initial bulk modulus
J	Ratio of the deformed volume over the reference volume
c_{01}, c_{10}	Mooney-Rivlin material constants
N, μ_i, α_i, d	Ogden material constants
N, c_{i0}, d_k	Yeoh material constants
λ	Stretch ratio
σ	Stress
ε	Strain

1. INTRODUCTION

In most solid rocket motors, thrust vector control (TVC) is required. By controlling the direction of the thrust vector by mechanical deflection of the nozzle, introduction of heat-resistant bodies in exhaust flow, injection of fluid in the nozzle divergent section, it is possible to control vehicles' pitch, yaw, and roll motions. The thrust vector control concept can be applied to both an engine or motor with single nozzle and for those that have two or more nozzles.

For large solid rocket motors (above 500 mm in diameter with 10 s of operation), secondary injection thrust vector control, fin tip control, flex nozzle / movable nozzles (hinged

by a flexible bearing, a ball and socket, or a hydraulic bearing joint) are mainly used as TVC¹ mechanisms. The flexible bearing is the most widely used device in modern nozzles for ballistic and space applications. The flex nozzle system offers advantages of efficiency, low reduction of thrust, and specific impulse. The moulded, multi-layer bearing acts as a seal², load transfer bearing, and a visco-elastic flexure. It uses the deformation of stacked set of curved elastomeric (rubbery) layers between spherical metal or composite sheets to carry the loads and permit angular deflections of the nozzle axis. A typical flex nozzle system, for which analysis is done, is shown in Fig. 1.

The elastomer selected should have certain specific properties. The joint spring torque is directly proportional to the elastomer shear modulus. So the elastomer should have as low a shear modulus as possible. The shear stress in the material is caused by the motor pressure and vectoring. For high pressure and high thrust vectoring motors, the shear strength required should be as high as possible. In case of storable solid rocket motors, ageing plays a major role. The elastomer should have less effect on the mechanical properties due to ageing. Other desired properties are good bonding with the reinforcement material and reproducibility of all the properties. The reinforcement should have a high material yield and ultimate strength, ease of machining, availability of fabrication expertise and infrastructure and simple heat treatment cycle.

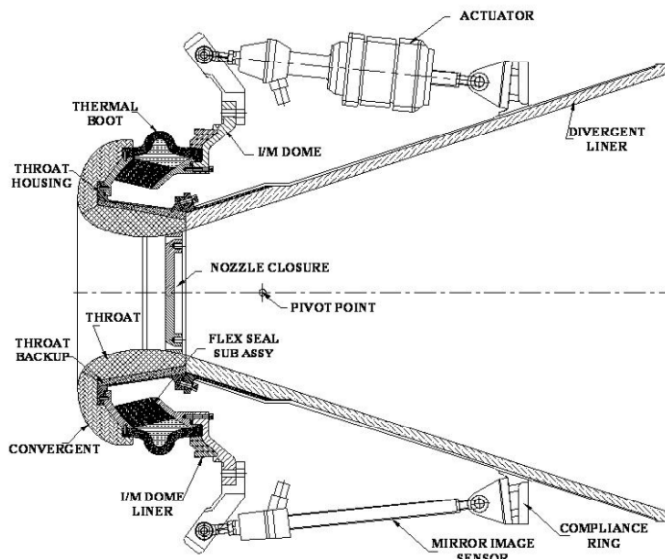


Figure 1. Typical flex nozzle system.

In the finite element analysis (FEA) of rubber engineering components, proper selection of a rubber elastic material model and the material parameters play an important role. The deformation state of these components is often a complex three-dimensional one. However, measurements of the mechanical behaviour are often performed for simple deformation states. Mooney-Rivlin model, Ogden model, Yeoh model, and Neo-Hookean model are the most widely used models among the classical rubber elasticity models. In this paper, the characterisation aspects of the natural rubber-based elastomer and AFNOR 15CDV6 reinforcement, developed for the use in flex bearing, are discussed.

2. MATERIAL CHARACTERISATION

2.1 Elastomer

The ingredients of the elastomer are natural rubber, carbon black filler, plasticiser, sulphur, accelerator and antioxidant. The elastomer is loaded in bulk compression and in shear direction during motor operation and vectoring of the nozzle. Material modelling of the elastomer requires data in all loading modes in which the elastomer is actually getting loaded during the rocket motor operation. For this, the elastomer is tested in tensile and shear directions. The mechanical properties of the elastomer are

Shear modulus at 0.343 MPa shear stress	: 0.245 MPa
Ultimate shear strength	: 2.65 MPa
Ultimate shear strain	: 800 % (min)
Hardness shores A (Max)	: 40

Tensile test on the elastomer is carried out using a dumbbell specimen as per ASTM D412. The specimens are shown in Fig. 2. The shear strength and shear modulus are evaluated using quadruple lap shear specimen (QLSS) as per BS 903 Part A14. The specimens are shown in Fig. 3. Stress versus strain curves for tensile test and QLSS for three specimens are given in Figs 4 and 5, respectively.

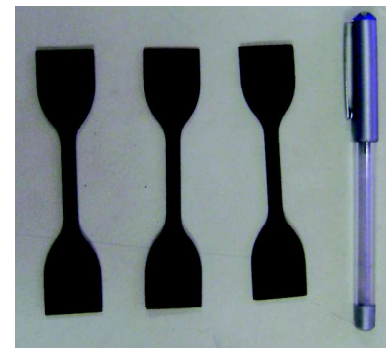


Figure 2. Tensile test specimen-elastomer.

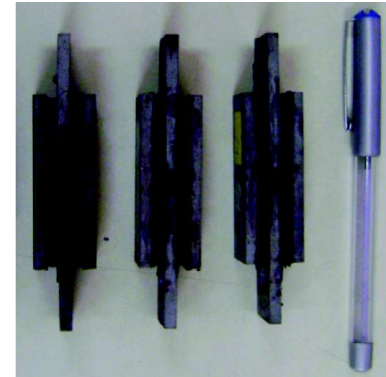


Figure 3. QLSS test specimen-elastomer.

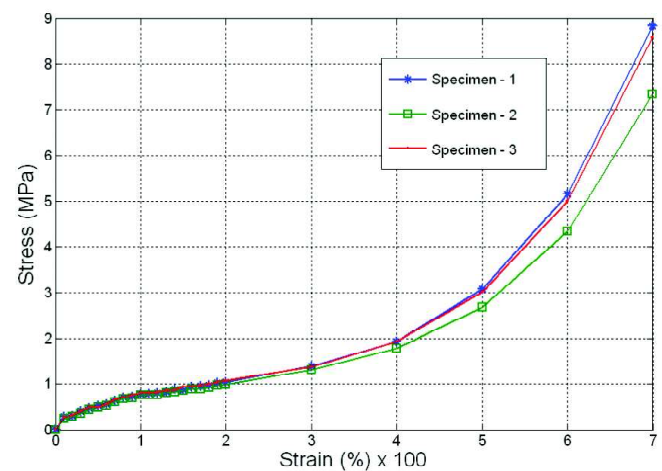


Figure 4. Stress vs strain for tensile test specimen-elastomer.

The failure modes in the elastomer, reinforcement combinations are adhesive bond failure and cohesive elastomer failure. The bond strength for the chosen adhesive system of Chemlok 205 and 220 is 40 Ksc (3.92 MPa) minimum and shear strength is about 27 Ksc (2.65 MPa). By design, the failure occurs within the elastomer (cohesive). To ensure this all the failures in the QLSS specimen must be cohesive¹ during testing at specimen level.

2.2 Reinforcement Material

The reinforcement material used in the flex seal is AFNOR 15CDV6 steel. The basic constituents of the material are carbon (0.15 per cent), chromium (1.5 per cent), molybdenum

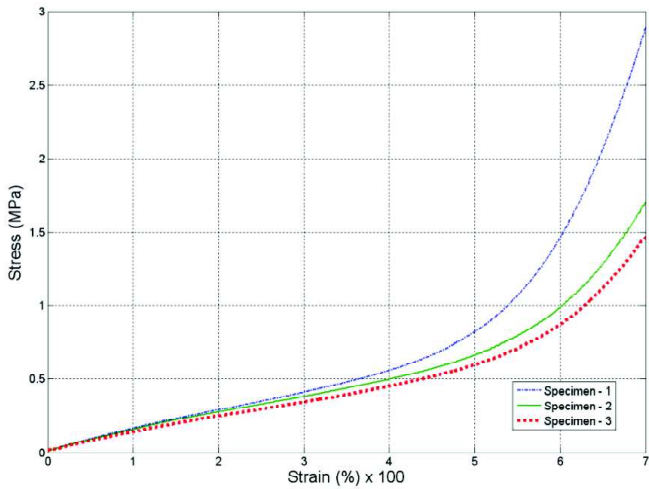


Figure 5. Stress vs strain for QLSS specimen-elastomer.

and vanadium (put together 1.5 per cent). The reinforcement is also loaded in bulk compression and in shear direction during motor operation and vectoring of the nozzle. The reinforcement experiences compressive hoop stresses on the ID which are dominating than the other components of stresses. The heat treatment cycle is given in Table 1. The mechanical properties of the reinforcement are:

- Ultimate Tensile Strength (MPa) : 980
- 0.2 per cent Proof stress (MPa) : 834
- Young’s Modulus (GPa) : 206
- Per cent elongation (min) : 10

The reinforcement material is characterised by carrying out tensile test on the specimen as per ASTM A 370 - 92. The specimens are shown in Fig. 6. Stress vs strain curve for three tested specimens are shown in Fig. 7.

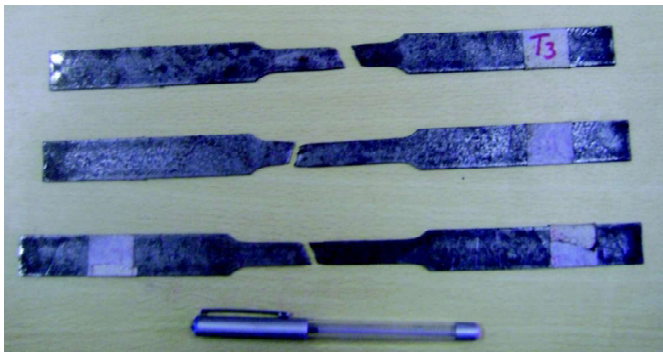


Figure 6. Tensile test specimen-reinforcement.

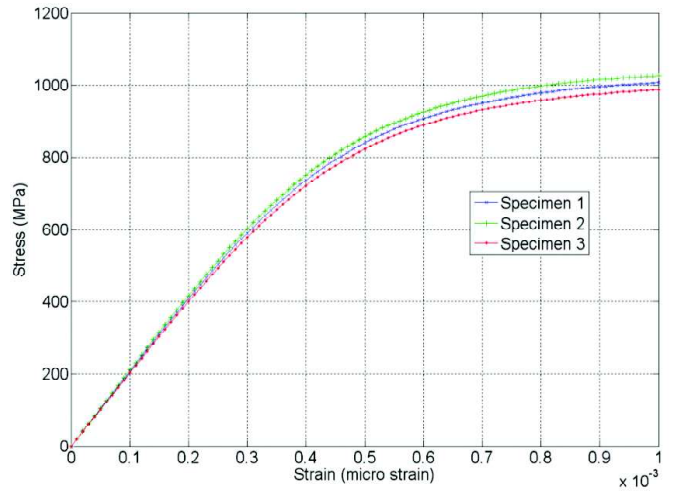


Figure 7. Stress vs strain curve for tensile tests-reinforcement.

3. MATERIAL MODELLING

3.1 Elastomer

For modelling elastomer, four material models, viz., Mooney-Rivlin, Neo-Hookean, Yeoh and Ogden material models are considered.

Mooney-Rivlin³⁻⁵ model exhibits a constant shear modulus and gives good correlation up to 150 per cent strain in uniaxial tension. In-house experimental data shows good match up to 200 per cent strain. The form of strain energy potential for 2-parameter model is

$$W = c_{10}(\bar{I}_1 - 3) + c_{01}(\bar{I}_2 - 3) + \frac{1}{d}(J - 1)^2 \quad (1)$$

$$K = \frac{2}{d}$$

A Neo-Hookean³⁻⁵ material model exhibits a constant shear modulus and gives good correlation with experimental data up to 40 per cent strain in uniaxial tension and up to 90 per cent in simple shear. However the elastomer developed and tested for this purpose shows good match between 80 per cent to 120 per cent strain and deviating in other regions. The strain energy potential for Neo-Hookean material model is

$$W = \frac{\mu}{2}(\bar{I}_1 - 3) + \frac{1}{d}(J - 1)^2 \quad (2)$$

Literature shows that the Ogden³⁻⁵ material model gives good correlation with test data in simple tension up to 700 per cent. It also accommodates non-constant shear

Table 1. Heat-treatment cycle for AFNOR 15CDV6

Treatment	Temperature, (°C)	Soaking time	Cooling medium
Annealing	875 ± 10	4 min/mm	Furnace cooling at the rate of 50 °C/h to room temperature
Hardening	875 ± 10	4 min/mm (or 20 min min)	Oil quench
Tempering	875 ± 10	8 min/mm (or 30 min min)	Oil quench

modulus and slightly compressible material behaviour. In-house experiments show a deviation from 80 per cent strain onwards. The form of strain energy potential is

$$W = \sum_{i=1}^N \frac{\mu_i}{\alpha_i} \left(\bar{\lambda}_1^{\alpha_i} + \bar{\lambda}_2^{\alpha_i} + \bar{\lambda}_3^{\alpha_i} - 3 \right) + \sum_{k=1}^N \frac{1}{d_k} (J-1)^{2k} \quad (3)$$

The Yeoh³⁻⁵ model has been demonstrated to fit various modes of deformation using data from a uniaxial tension test only. This model should be used with caution at low strains. However, in-house experiment shows the behaviour similar to Neo-Hookean model. The strain energy potential is

$$W = \sum_{i=1}^N c_{i0} \left(\bar{I}_1 - 3 \right)^i + \sum_{k=1}^N \frac{1}{d_k} (J-1)^{2k} \quad (4)$$

The comparison^{5,6} of the experimental data with all the four material models is given in Fig 8. It is clearly evident that Mooney-Rivlin and Ogden material models are having a good correlation with experimental data. The percentage variation of Mooney-Rivlin and Ogden material models wrt experimental data is 4.94 per cent and 9.75 per cent, respectively. From the practical usage point of view, deformation of elastomer for the pressure loading is of the order of 30-40 per cent in compression and deformation due to shear being of the order of 100-150 per cent. Based on these conditions, the Mooney-Rivlin model was been selected to simulate the elastomer.

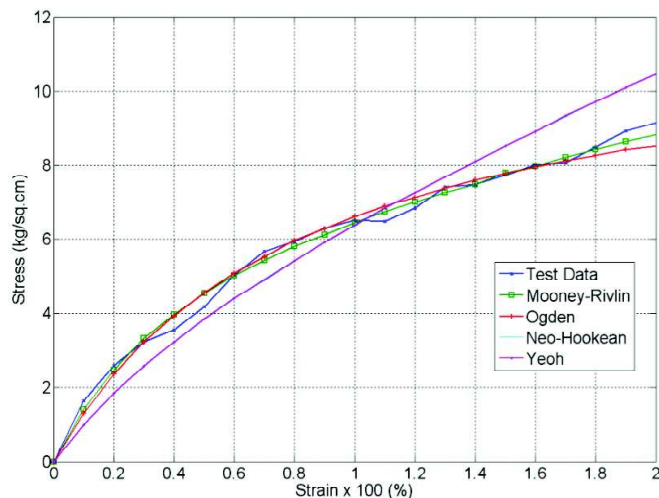


Figure 8. Comparison of material models.

4. MATERIAL CONSTANTS EVALUATION

4.1 Elastomer

The constants of the materials were derived using experimental stress-strain data. It is recommended that this test data be taken from several modes of deformations over a wide range of strain values. To achieve material stability, the constants should be fit using test data in at least as many deformation states as will be experienced in the model.

For characterising hyperelastic materials, six different deformation modes can be used. These are uniaxial tension, uniaxial compression, equibiaxial tension, equibiaxial compression, planar tension, and planar compression. Combinations of data from multiple tests will enhance the characterisation of the hyperelastic behaviour of the material⁷.

Once the strain energy function is defined, the stress is obtained by differentiating the strain energy wrt to the strain as

$$\sigma = \frac{\partial W}{\partial \varepsilon} \quad (5)$$

For an incompressible material in uniaxial tensile state, the volume change due to deformation is zero and the ratio of original to deformed configuration volume is one. This can be represented as the third invariant of strain $I_3 = 1$, i.e.,

$$\lambda_1^2 \lambda_2^2 \lambda_3^2 = 1 \quad (6)$$

These results are incorporated into the strain energy function considering the case of a rubber rod subjected to uniaxial tension along its longitudinal axis. Let λ_1 be the stretch ratio along the longitudinal axis and λ_2 and λ_3 be the stretches along the lateral axes. For uniaxial tension, the deformation state is represented,

$$\lambda_1 = \lambda \quad (7)$$

and,

$$\lambda_2 = \lambda_3 = \frac{1}{\sqrt{\lambda}} \quad (8)$$

By differentiating the strain energy potential and substituting the above expressions, the stress for a two-parameter Mooney-Rivlin model is^{8,9}

$$\sigma = 2 \left(\lambda - \frac{1}{\lambda^2} \right) \left(C_{01} - \frac{C_{10}}{\lambda} \right) \quad (9)$$

A similar procedure is adopted to derive the relations for other material models. The material constants for all the models are given in Table 2.

Table 2. Material constants of elastomer models

Material Model	Constants
Mooney-Rivlin [Eqn (1)]	$C_{01} = 0.92029$ & $C_{10} = 1.8434$
Ogden [Eqn (2)]	$\mu = 8.5090$ & $\alpha = 1.1537$
Neo-Hookean [Eqn (3)]	$\mu = 1.81806$
Yeoh [Eqn (4)]	$\mu = 1.81806$

The plot of $\frac{\sigma}{2} \left(\lambda - \frac{1}{\lambda^2} \right)$ vs. $\frac{1}{\lambda}$ gives a straightline

(Fig. 9) with slope c_{10} and intercept c_{01} .

For analysis of the elastomer in axial compression, data from uniaxial tensile test data is used. For analysis of the rubber in both axial compression and vectoring mode, uniaxial tensile data is not sufficient to predict the behaviour of the elastomer. Mooney-Rivlin model has to be fitted by having uniaxial tensile data and shear data.

The plot of uniaxial test data and shear test data are fitted with experimental data for two-parameter Mooney-Rivlin model and is shown in Fig. 10.

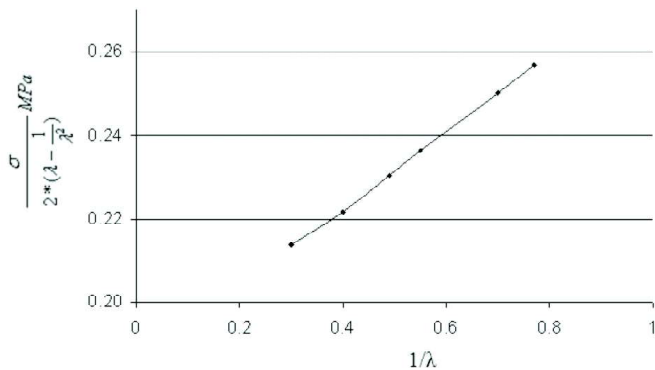


Figure 9. Mooney-Rivlin constants for elastomer.

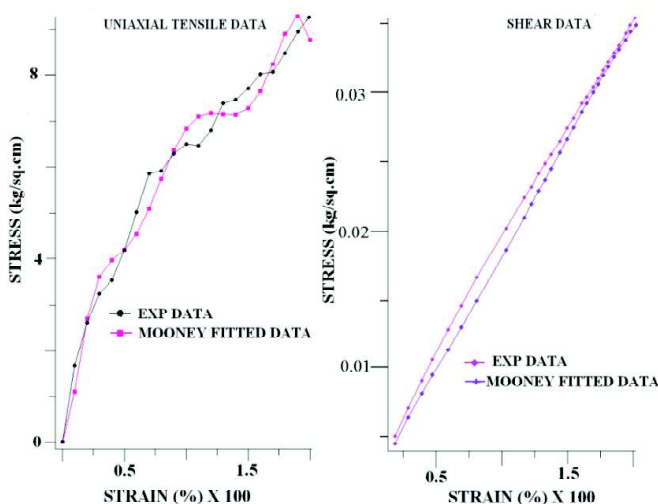


Figure 10. Two-parameter mooney Rivlin model.

4.2 Reinforcement

The design criteria for flex bearings are the margin of safety to be lower among 0.125 on yield strength and 0.25 on ultimate tensile strength. The design is carried out to have a working stress close to yield strength of the material. The material is not linear all through the stress-strain curve.

The need for modelling the reinforcement material as a multi-linear elastic material model arises because of the working stresses close to yield strength of the material. The model considers constant Young's modulus between two points on the stress-strain curve. To have a better approximation, stress at every 100 μ strains data has been taken into account.

5. VALIDATION OF MATERIAL MODELS

The material models have to be validated before using these in analysis. The validation of the material models with the test data is done by modelling the test specimens in ANSYS and loading is applied in steps to get the strain induced¹⁰⁻¹³.

The stress-strain curve for every 100 μ strains of the reinforcement material is given as input for metal. The FE model is shown in Fig. 11 and the deflection plot for a load of 25 N is shown in Fig. 12. The comparison of the results between FEM and the test data is shown in Fig. 13. The curve clearly shows a good match up to 400 per cent elongation for two-parameter Mooney-Rivlin material model. The shear stress in the elastomer for failure load is more than the shear strength of the material which is observed in the corners of the elastomer metal combination. The corner stresses on the elastomer are neglected because of stress singularity.

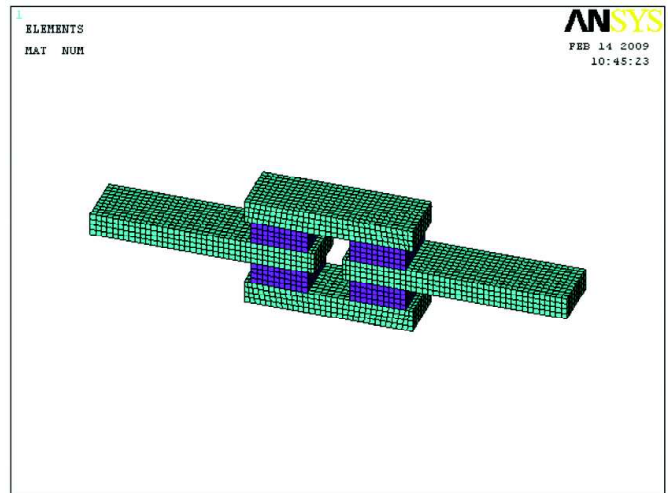


Figure 11. FE model of the QLSS specimen.

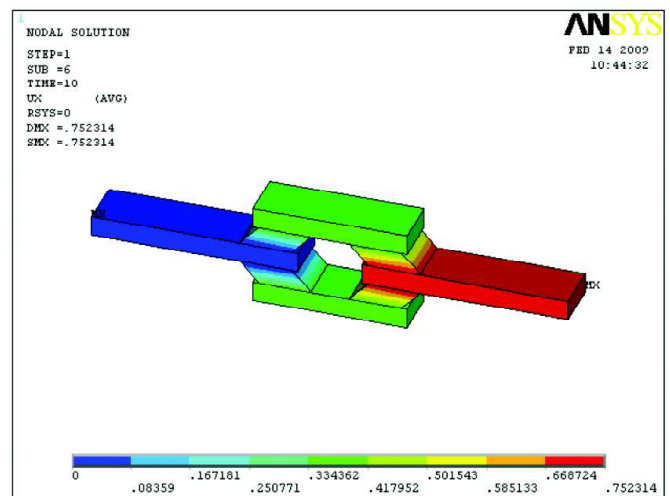


Figure 12. Displacement plot of a QLSS specimen.

6. CONCLUSIONS

The material characterisation of elastomer and reinforcement shims used in flex bearings of solid rocket motors are carried out. The hyper-elastic modelling of elastomer was studied with four material models and two-parameter Mooney-Rivlin model was found to be the most suitable model for modelling the flex bearing. The material models are validated at the specimen level. The predictions

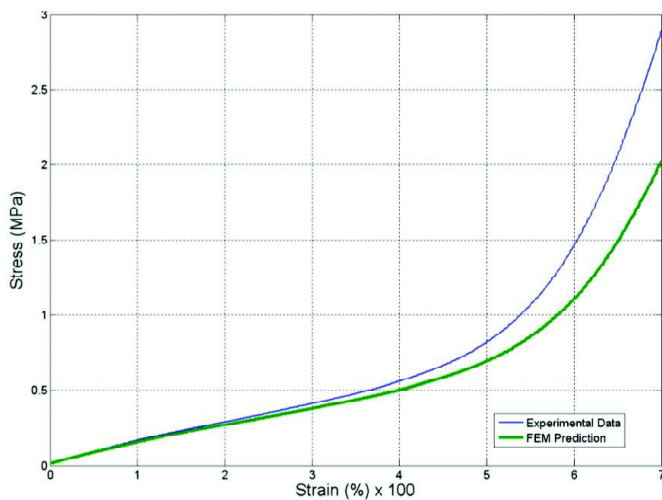


Figure 13. Comparison of FEM predictions and experimental results for a QLSS specimen.

from the models are having a very close match with the test data. The model-fitted data varies within 10-11 per cent wrt the experimental data.

REFERENCES

1. Woodberry, Robert H.F. Solid rocket thrust vector control. NASA SP-8114, December 1974, 4-17.
2. Solid rocket motor nozzles, NASA SP-8115, June 1975, 70 p.
3. Boyce, Mary C. & Arruda, Ellen M. Constitutive models of rubber elasticity: A review. *Rubber Chem. Technol.*, 2000, **73**(3), 504-23.
4. Ghosh, P.; Asaha, & Bohara, P.C. Material property characterisation for finite element analysis of tyres. *Rubber World*, 2006, 22-31.
5. Riande, *In* Polymer viscoelasticity. Marcel Dekker Inc. New York, 2000, pp. 101-09.
6. Seibert, D.J. & Schoche, N. Direct comparison of some recent rubber elasticity models. *Rubber Chem. Technol.*, 2000, **73**(2), 366-84.
7. Ansys: Theoretical Reference Manual. Version 6.0, Chapters 3 & 4.
8. Valanis, K.C. The strain energy function of a hyperelastic material in terms of the extension ratio. *J. App. Phy.*, 1967, **38**(7), 2997-3002.
9. Sivaramkrishnan, R. & Bhagawan, S.S. Characterisation of natural rubber-based flex nozzle material for solid rocket motors. *In* IRMRA 15th Rubber Conference, India, 1992. pp. 221-30.
10. Wang, Li-Rong & Lu, Zhen-Hua. Modelling method of constitutive law of rubber hyperelasticity based on finite element simulations. *Rubber Chem. Technol.*, 2003, **76**(2), 271-85.
11. Yeoh, O.H. Some benchmark problems for FEA from torsional behaviour of rubber. *Rubber Chem. Technol.*, 2003, **76**(3), 1212-227.
12. Martinsz, Pedro A.L.S.; Jorgex, Renato M. Natal & Ferreiray, Antonio J.M. Determination of material

parameters for different hyperelastic models. *In* Proceedings of 8th International Conference on Computational Plasticity, 2005. pp.1-4.

13. Amin, A.F.M.S.; Wiraguna, S.I.; Bhuiyan, A. R. & Okui, Y. Hyperelasticity model for finite element analysis of natural and high damping rubbers in compression and shear. *J. Engg. Mech.*, 2006, **132**(1), 54-64.

Contributors



Mr CH V. Ram Mohan obtained his BE from Osmania University, and MS from JNTU, Hyderabad and completed one year fellowship programme at DIAT, Pune. Presently working as Scientist 'F', Deputy Project Director at the Advanced Systems Laboratory (ASL), Hyderabad. His main interests are design and development of large solid rocket motors especially with flex nozzle systems and airframe design for ballistic missiles. He has been awarded *DRDO Laboratory Scientist of the Year-2002*, and *Agni Award for Excellence in Self Reliance-2005* as a team member.



Mr J. Ramanathan obtained his BTech from Madras Institute of Technology, Chennai. Presently, he is working as Scientist 'C' in Solid Propulsion Systems Centre at ASL, Hyderabad. He has been working in the area of flex nozzle-based thrust vector control systems. His area of interests includes structural analysis, aerospace structures.



Dr Sathish Kumar obtained his BE from Punjab Engineering College, Chandigarh, and MTech (Aero) from IIT, Kanpur in 1980 and 1982, respectively. He did his PhD (Mechanical Engineering) from REC, Warangal, in 1996. Presently, he is working as Director, Terminal Ballistics Research Laboratory, Chandigarh. He was associated with the design and development of liquid propellant rocket engines for Prithvi and Agni Missiles and cold and hot gas reaction control systems for Prithvi and Agni variants. He was also involved in the design and development of liquid propellant storage facilities and propellant transfer systems for Prithvi missiles.



Dr A.V.S.S.K.S. Gupta obtained his BTech (Mech. Engg.) from JNTU College of Engineering, Ananthapur, MTech from NIT, Warangal, and PhD from IIT, Kharagpur. Presently, he is working as Associate Professor of Mechanical Engineering, JNTU College of Engineering, Hyderabad. He published 50 papers in various international and national journals and Conferences. His research areas include finite element analysis and thermal analysis.